Journal of Materials Chemistry C

Accepted Manuscript

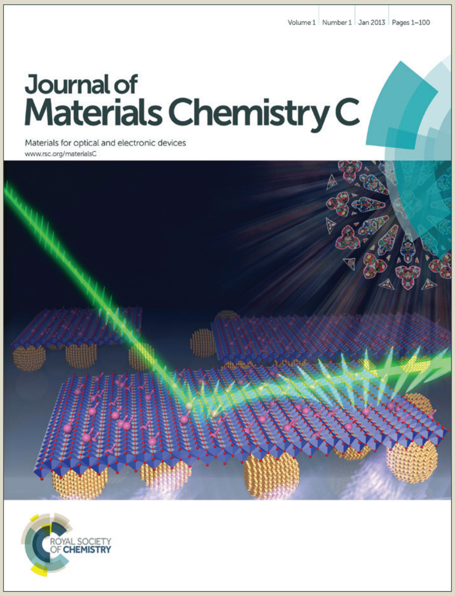

ROYAL SOCIETY OF CHEMISTRY

www.rsc.org/materialsC

Cite this: DOI: 10.1039/c0xx00000x

www.rsc.org/xxxxxx

ARTICLE TYPE

Sub-millimeter free-suspended sheets formed by polyoxometalates with polyelectrolytes

Nijuan Liu, Hui Wang and Weifeng Bu*

Received (in XXX, XXX) Xth XXXXXXXXX 20XX, Accepted Xth XXXXXXXXX 20XX
DOI: 10.1039/b000000x

The electrostatic combination of cationic polyelectrolytes with polyoxometalates in aqueous solution yields polyoxometalate-based free-suspended sheets with a planar-view size of sub-millimeter ranges and a nanoscale thickness.

Polyoxometalates (POMs) are anionic metal-oxide cluster with the structural, chemical, and electronic versatility and have many applications in the field of catalysis, energy storage, biomedicine, and surface coatings.[1] However, they are highly hydrophilic and have high lattice energies associated with crystallization. Therefore, these clusters can be regarded as unprocessable materials. To their above-mentioned applications, POMs can be readily manipulated at nanoscale to fabricate functional POM-based hybrids through electrostatic self-assembly with cationic polymers in solutions.[2] The resulting hybrids can be further self-assembled to form hierarchical nanostructures, such as nanowires,[2a,b] micelles,[2c–g] and vesicles,[2c–e,g,h] as well as highly ordered hexagons[2c,d,g] and porous nanocomposites[2i,j]. These nanostructures are proposed to be highly relevant to the functional performance in catalysis and materials science. Although above zero-dimensional, one-dimensional and three-dimensional POM-based hybrids have been reported, the existence of POM-based two-dimensional sheet important for potential applications has not been demonstrated.

In order to prepare such anisotropic nanostructures, the organic counter-multi-cations should bind directionally with POMs by cooperative electrostatic interactions. However, it is well-known that the coulomb interaction has no selectivity between the ionic partners. Polyelectrolytes are polymers whose repeating units contain an electrolyte group.[3] The charges on a linear polyelectrolyte chain will repel each other by Coulomb repulsion. This induces the chain to adopt a relatively expanded, rigid-rod-like conformation in aqueous solution. Recently, the alternating electrostatic deposition of POMs with cationic polyelectrolytes on the substrate surface leads to POM/polyelectrolyte hybrid ultrathin films.[4] Furthermore, POM-based vesicles were formed by electrostatic incorporation of POMs into amphiphilic block copolymers.[2c,d,g] Combining these features together, we here describe the electrostatic combination of POMs and cationic polyelectrolytes to yield POM-based free-suspended sheets with sub-millimeter sizes through solution-based self-assembly.

A typical procedure for preparing the free-suspended sheets was described as follows. Poly(*p*-xylene tetrahydrothiophenium chloride) (PXTT, Adrich, Fig. 1), was added into an aqueous solution of α-tungstosilicate acid (α-$H_4SiW_{12}O_{40}$, TSA, Aldrich, 0.15 mmol/L, Fig. 1) with vigorous stirring, in which the final charge ratio of PXTT (based on the repeated unit) against TSA was controlled at 1/1. Pale yellow suspension formed, which was further stirred for 3 h for fully electrostatic interactions. The suspension was cast onto various substrates for spectroscopic and microscopic measurements.

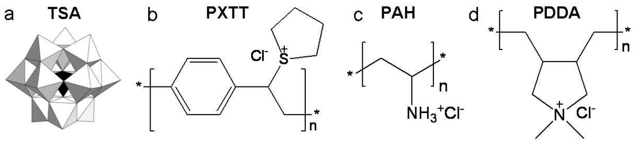

Fig. 1 Chemical structures of ionic building blocks used this study.

In infrared spectrum of the mixture, bands at 973, 922, 883, and 795 cm^{-1} are associated with $[SiW_{12}O_{40}]^{4-}$ (Table S1). These bands showed slight shifts in comparison with those of $H_4[SiW_{12}O_{40}]$ (981, 928, 880, and 785 cm^{-1}). Such shift means that PXTT cations have a strong interaction with $[SiW_{12}O_{40}]^{4-}$ and partly screen the interanionic repulsions.[5]

Fig. 2 showed various microscopic images of the nanocomposites formed by PXTT and TSA. Laser optical microscopy (LOM) images (Fig. 2a, bright field, and Fig. 2b, dark field) indicated that a free-suspended sheet formed with a planar-view size of 110 µm. The formation of the sheets was further confirmed by both scanning electron microscope (SEM) and transmission electron microscope (TEM) (Fig. 2c and 2d). In these images, the sheets appeared as wrinkled platelets, and even were occasionally folded into bilayers (Fig. S1a). Such observations demonstrated that the two-dimensional sheets formed in the aqueous solution rather than on the substrate during the drying process. Both the SEM and TEM observations at high magnifications didn't show any pore in the sheets, indicating a rather compact packing of TSA clusters with PXTT. The thickness of the sheets was estimated to be 40 ± 10 nm by the cross-sectional SEM (Fig. 2e), which was much larger than the sum of the diameter of TSA (1.04 nm) and the width of PXTT (0.66 nm). Therefore, the sheets corresponded to the bundled PXTT/TSA complexes. Fig. 2f shows a high-resolution TEM image, where the TSA clusters were well-discerned and homogeneously dispersed into the sheets. In several SEM measurements, we sporadically observed nanofibers with a length of a few tens of micrometers and a width of a few tens of nanometers (Fig. S1a). Based on the microscopic observations above, we therefore estimated that more than 98% of PXTT and TSA assembled into the sheets by the electrostatic interactions. In contrast to the relative uniformity of the thickness, the sheets showed a broad range of planar-view sizes from 80 to roughly 300 μm (Fig. S2). However, such a big anisotropic growth for two-dimensional entities occurred on the basis of a programmably electrostatic self-assembly of commercially-available cationic polyelectrolytes with opposite-charged multivalent clusters. Furthermore, the concentration-dependent preparations of the sheets (5–30 μmol/L of TSA) didn't show a big difference in the size and morphology. The sheet-like materials exhibited a strong emission with a λ_{max} of 473 nm, which showed a significant red-shift in comparison with that of PXTT in its dilute solution (λ_{max} = 442 nm, Fig. S3).

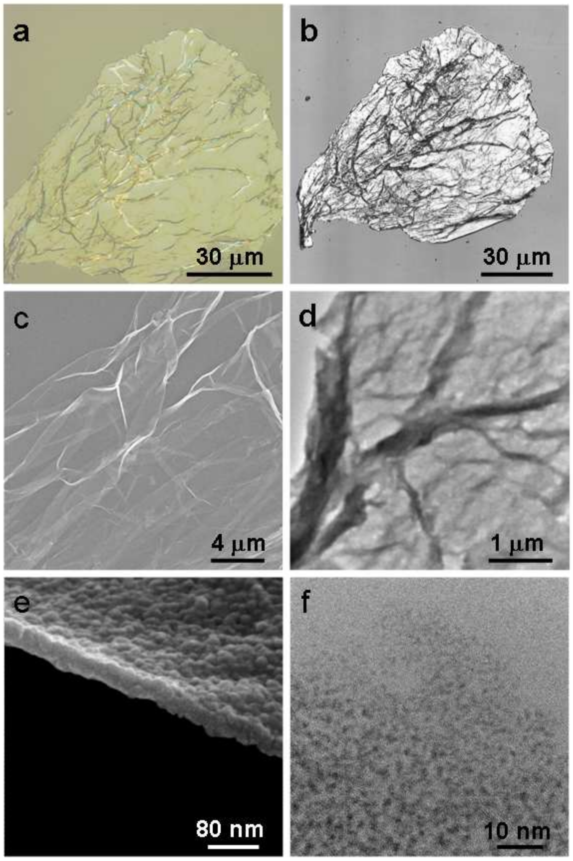

Fig 2. Microscopic observations of the free-suspended films formed by PXTT and TSA: (a) bright field and (b) dark field images of LOM, (c) SEM image, (d) TEM image, (e) cross-sectional image, and (f) high-resolution TEM image.

This discovery raised an interesting question concerning how to understand the mechanism of the sheet formation. For this purpose, SEM experiments were carried out at different stirring stages. The images at initial stages showed nanofibers and bundling nanofibers (Fig. S4), which should be due to a rapid electrostatic self-assembly at the interface between the two liquids of the aqueous solutions of TSA and PXTT. When the stirring time was prolonged to 50 min, Fig. 3a captured a length of nanofibers in the act of both longitudinal and lateral spreading (arrows); they had not yet resulted in the fully expanded sheets. A further increase in stirring time to 90 min revealed much more expanded sheets (Fig. 3b). After stirring for 3 h, the SEM images showed total POM-based sheets with a planar-view size of sub-millimeter ranges and a nanoscale thickness (Fig. 2). On the basis of the time-dependent SEM results, the nanofibers were firstly broken up by TSA clusters with the electrostatic interactions, and then grew into the free-suspended sheets by both the longitudinal and lateral directions (Fig. 3c and 3d). In this growth process, the electrostatic interactions between TSA and PXTT should be directional.

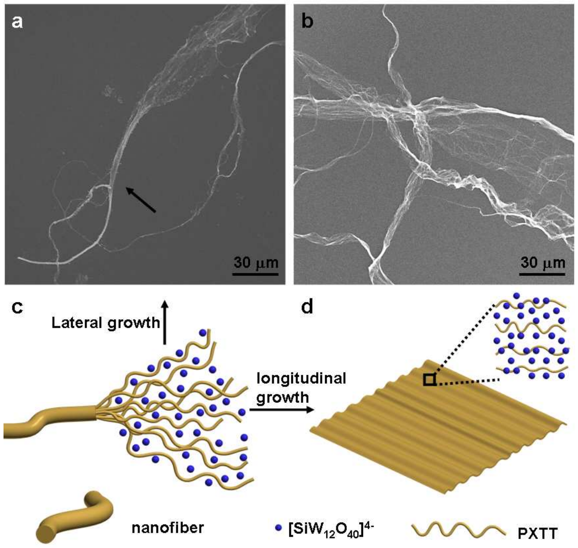

Fig 3. SEM images of the nanocomposites formed by PXTT and TSA cluster after stirring for 50 min (a). The arrow in (a) showed nanofibers in the act of both longitudinal and lateral spreading. Much more expanded sheets were observed by using SEM after stirring for 90 min (b). Schematic illustrations demostrated a two-dimensional growth process for the sheet formation (c and d).

For comparison, we prepared POM-based nanocomposites of poly(allylamine hydrochloride) (PAH, Aldrich, M_w, 15,000) and poly(diallyldimethylammonium) chloride (PDDA, Aldrich, M_w: 400,000-500,000) with TSA clusters (Fig. 1). Both SEM and TEM images of the PAH/TSA nanocomposites revealed cross-linked nanofibers with a width of 16-20 nm (Fig. S5). Similar situation is also observed in the case of PDDA/TSA nanocomposites. These results indicated that only a longitudinal growth was present in PAH/TSA and PDDA/TSA partners. However, both longitudinal and lateral growth processes were captured for the sheet formation of PXTT/TSA partners. Fundamentally, electrostatic interactions between oppositely charged species are nondirectional.[6] $[SiW_{12}O_{40}]^{4-}$ is a spherical POM anion with high symmetry of T_d.[5] It is believed that the four negative charges are homogenously distributed on the globular surface. Therefore, the remarkable difference of the above-described morphologies should be attributed to the much more expanded and rigid conformation of PXTT than that of PAH and PDDA. Consequently, the cationic charges are laterally distributed along the semi-rigid PXTT chains, which induces directional electrostatic interactions with TSA clusters and thus leads to the two-dimensional growth of the free-suspended sheets.

In order to further test the two-dimensional growth mechanism that originated from the anisotropic electrostatic interactions induced by molecular shapes, phthalocyanine tetrasulfonate acid (PTA, 1.3×1.3×0.35 nm^3, Fig. 4a) was chosen as a geometrically different building block to fabricate the corresponding nanocomposite with PXTT. PTA is a flat molecule with four negative charges, of which both molecular volume and charged number are consistent with TSA cluster. Of different is that the four negative charges of PTA are diagonally distributed within the molecular square plane, which is a sharp contrast to the isotropic distributions of the charges on the surface TSA. Accordingly, the PXTT/PTA partners should have much more anisotropic electrostatic interactions than the PXTT/TSA ones. We therefore predicted here that the PXTT/PTA sheets will show the larger planar-view size, the thinner thickness and much larger aspect ratio than the PXTT/TSA opponents.

By applying the same procedure, we obtained the blue free-suspended sheets of PXTT with PTA. Fig. 4b features a wrinkled and folded sheet by bright-field LOM. Considering the folded part (arrows), this blue sheet had a planar-view size of roughly 880 µm, which was much larger than that of the PXTT/TSA counterpart. The magnified SEM image (Fig. 4c) showed a relatively flat surface in comparison with that of the PXTT/TSA sheets. Fig. 4d showed a cross-sectional image for which the observed thickness of the sheets was 30 ± 5 nm. The PXTT/PTA sheets were thinner than those formed by PXTT and TSA. On the basis of these data, we estimated an aspect ratio of approximately 30,000 for the PXTT/PTA sheets. These results were in good agreements with the above-mentioned predictions, which further supported the postulated mechanism that the sheet formation stems from the directional electrostatic interactions induced by the molecular shapes/conformations of ionic building blocks.

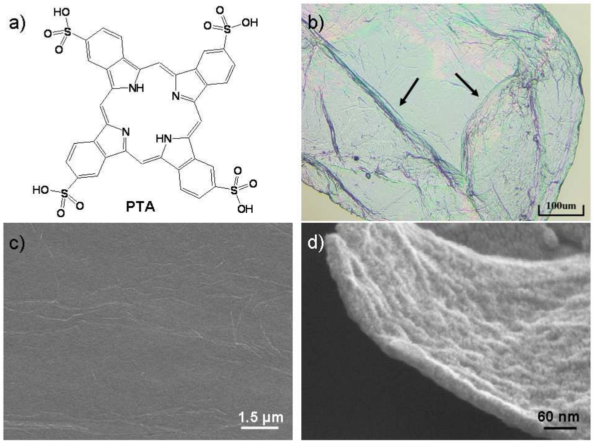

Fig. 4 a) The chemical structure of PTA. b) LOM bright field, c) SEM and (d) cross-sectional SEM images of the free-suspended films formed by PXTT and PTA.

Tungstophosphoric acid (TPA, $H_3[PW_{12}O_{40}]$, 1.04 nm)[5a] has 3 negative charges and an almost consistent Keggin-type structure with $H_4[SiW_{12}O_{40}]$. When this Keggin anion was similarly mixed with PXTT, we also obtained the pale-yellow free-suspended sheets as indicated in the SEM and TEM images (Fig. S6a and b). The TPA clusters were clearly observed in the magnified TEM images (Fig. S6c). The Keplerate cluster of $(NH_4)_{42}[Mo_{132}O_{372}(CH_3COO)_{30}(H_2O)_{72}]\bullet(H_2O)_{300}\bullet(CH_3COONH_4)_{10}$ (Mo_{132}) is a nearly spherical nanocapsule with a diameter of 2.8 nm and 42 negative charges.[7] However, the electrostatic self-assembly of this cluster with PXTT resulted in the formation of sponge-like nanopores (Fig. S6e, f and g). This porous nanostructure was totally different from the sheet-like assemblies fabricated by PXTT with TSA, TPA, or PTA. This should be due to the much larger size and charge number in the spherical Keplerate cluster that led to almost isotropic electrostatic interactions with PXTT.

Recently, several reports concerned the sheet formation through a bottom up self-assembly in solution.[8] For example, nanoparticles spontaneously formed two-dimensional free-floating sheets in solution driven by combining anisotropic hydrophobic attraction with anisotropic electrostatic interactions induced by both a dipole moment and a small positive charge.[8a] The coordination combination of conjugated polymers with porphyrin-based bidirectional "clips" produced the ordered sheets.[8b,c] Dumbbell-shaped rod amphiphiles self-assembled into nanoporous sheets in aqueous solution driven by a fine balance of anisotropic hydrophobic interactions and steric constraints endowed with bulky dendritic wedges.[8d] These sheets were monolayers or bilayers and the planar-view sizes were usually smaller than 50 µm.

Our results illustrated that the electrostatic combination of semi-rigid cationic polyelectrolytes with POMs in aqueous solution yielded free-suspended sheets, of which the planar-view size reached sub-millimeter ranges. Furthermore, the sheets formed by PXTT and PTA had a planar-view size of almost 1 mm. These findings were attributed to the anisotropic electrostatic interactions induced by the molecular shapes/conformations of ionic building blocks.[9] Considering highly available POMs and oppositely charged polyelectrolytes, the controlled preparation of the giant free-suspended sheets represents a new strategy for the design of POM-based two-dimensional materials with integrated functions such as nanoseparation and electro-optics.

This work is supported by the NSFC (51173073), the Program for New Century Excellent Talents in University (NCET-10-0462) and the Open Project of State Key Laboratory of Supramolecular Structure and Materials of Jilin University (sklssm201405).

Notes and references

Key Laboratory of Nonferrous Metals Chemistry and Resources Utilization of Gansu Province, State Key Laboratory of Applied Organic Chemistry, and College of Chemistry and Chemical Engineering, Lanzhou University, Lanzhou City, Gansu Province, China, Fax: +86 931 8912582; Tel: +86 931 8912265; E-mail: buwf@lzu.edu.cn

† Electronic Supplementary Information (ESI) available: Intruments and additional SEM images for the fibers and free-suspended sheets. See DOI: 10.1039/b000000x/

‡ Footnotes should appear here. These might include comments relevant to but not central to the matter under discussion, limited experimental and spectral data, and crystallographic data.

1 (*a*) C. L. Hill, *Chem. Rev.*, 1998, **98**, 1; (*b*) N. Mizuno, K. Yamaguchi and K. Kamata, *Coord. Chem. Rev.*, 2005, **249**, 1944; (*c*) N. Casañ-Pastor and P. Gómez-Romero, *Front. Biosci.*, 2004, **9**, 1759; (*d*) A. Proust, R. Thouvenot and P. Gouzerh, *Chem. Commun.* **2008**, 1837. (*e*) S. Liu and Z. Tang, *Nano Today*, 2010, **5**, 267; (*f*) D. Long, R. Tsunashima and L. Cronin, *Angew. Chem. Int. Ed.*, 2010, **49**, 1736.

2 (*a*) M. A. Alam, Y.-S. Kim, S. Ogawa, A. Tsuda, N. Ishii and T. Aida, *Angew. Chem. Int. Ed.*, 2008, **47**, 2070; (*b*) R. S. Yekamanchili, A. Walther, A. H. E. Müller and J. Breu, *Chem. Commun.*, 2008, 489; (*c*) W. Bu, S. Uchida and N. Mizuno, *Angew. Chem. Int. Ed.*, 2009, **48**, 8281; (*d*) Q. Zhang, Y. Liao, L. He and W. Bu, *Langmuir*, 2013, **29**, 4181; (*e*) Q. Zhang, Y. Liao and W. Bu, *Langmuir*, 2013, **29**, 10630; (*f*) X. Lin, F. Liu, H. Li, Y. Yan, L. Bi, W. Bu and L. Wu, *Chem. Commun.*, 2011, **47**, 10019; (*g*) T. Lunkenbein, M. Kamperman, Z. Li, C. Bojer, M. Drechsler, S. Förster, U. Wiesner, A. H. E. Müller and J. Breu, *J. Am. Chem. Soc.*, 2012, **134**, 12685; (*h*) Q. Zhang, L. He, H. Wang, C. Zhang, W. Liu and W. Bu, *Chem. Commun.*, 2012, **48**, 7067; (*i*) A. Haimov and R. Neumann, *J. Am. Chem. Soc.*, 2006, **128**, 15697; (*j*) A. Haimov, H. Cohen and R. Neumann, *J. Am. Chem. Soc.*, 2004, **126**, 11762; (*k*) D. Li, H. Li and L. Wu, *Polym. Chem.*, 2014, **5**, 1930.

3 (*a*) R. Podgornik and M. Ličer, *Curr. Opin. Colloid Interface Sci.*, 2006, **11**, 273; (*b*) A. Laschewsky, *Curr. Opin. Colloid Interface Sci.*, 2012, **17**, 56.

4 (*a*) I. Ichinose, H. Tagawa, S. Mizuki, Y. Lvov and T. Kunitake, *Langmuir*, 1998, **14**, 187; (*b*) F. Caruso, D. G. Kurth, D. Volkmer, M. J. Koop and A. Müller, *Langmuir*, 1998, **14**, 3462; (*c*) S. Liu, D. G. Kurth, B. Bredenkötter and D. Volkmer, *J. Am. Chem. Soc.,* 2002, **124**, 12279; (*d*) Y. Wang, X. Wang, C. Hu and C. Shi, *J. Mater. Chem.*, 2002, **12**, 703; (*e*) L. Xu, H. Zhang, E. Wang, D. G. Kurth and Z. Li, *J. Mater. Chem.*, 2002, **12**, 654.

5 (*a*) C. Rocchoccioli-Deltcheff, M. Fournier, R. Franck, R. Thouvenot, *Inorg. Chem.*, 1983, **22**, 207; (*b*) H. Li, H. Sun, W. Qi, M. Xu, and L. Wu, *Angew. Chem. Int. Ed.*, 2007, **46**, 1300; (*c*) A. Tézé and G. Hervé*Inorganic Synthesis*; John Wiley and Sons: New York, 1990.

6 (*a*) C. F. J. Faul and M. Antonietti, *Adv. Mater.*, 2003, **15**, 673; (*b*) I. Willerich and F. Gröhn, *Angew. Chem. Int. Ed.*, 2010, **49**, 8104.

7 A. Müller, E. Krickemeyer, H. Bögge, M. Schmidtmann and F. Peters, *Angew. Chem., Int. Ed.*, 1998, **37**, 3360.

8 (*a*) Z. Tang, Z. Zhang, Y. Wang, S. C. Glotzer and N. A. Kotov, *Science*, 2006, **314**, 274; (*b*) Y. Kubo, Y. Kitada, R. Wakabayashi, T. Kishida, M. Ayabe, K. Kaneko, M. Takeuchi and S. Shinkai, *Angew. Chem. Int. Ed.*, 2006, **45**, 1548; (*c*) R. Wakabayashi,; Y. Kubo, K. Kaneko, M. Takeuchi and S. Shinkai, *J. Am. Chem. Soc.*, 2006, **128**, 8744; (*d*) J.-K. Kim, E. Lee, Y.-H. Jeong, J.-K.Lee, W.-C. Zin, M. Lee, *J. Am. Chem. Soc.*, 2007, **129**, 6082.

9 Such cooperative electrostatic interactions were also used to fabricate nanotubes, nanowires and vesicles: (*a*) Z. Wang, C. J. Medforth and J. A. Shelnutt, *J. Am. Chem. Soc.*, 2004, *126*, 15954; (*b*) T. Shiraki, M-a. Morikawa and N. Kimizuka, *Angew. Chem. Int. Ed.*, 2008, **47**, 106; (*c*) F. Gröhn, K. Klein and K. Koynov, *Macromol. Rapid Commun.*, 2010, **31**, 75.

Graphical Abstract

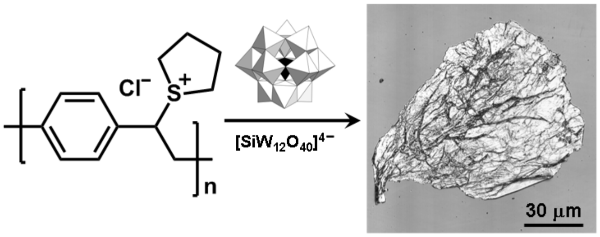

Sub-millimeter free-suspended sheets formed by polyoxometalates with polyelectrolytes

Nijuan Liu, Hui Wang and Weifeng Bu*

Electrostatic self-assembly of polyoxometalates with cationic polyelectrolytes yields sub-millimeter free-suspended sheets with a nanoscale thickness.